Improved detection of thermally induced higher resonance modes and harmonics of a microcantilever

A. K. Kar and M. A. George[a)]
The Laboratory for Materials and Surface Science, Materials Science Program, University of Alabama in Huntsville, Huntsville, Alabama 35899

(Received 8 April 2003; accepted 8 July 2003)

Driving a microcantilever externally may not be desirable in many sensor applications. Alternatively, it is possible to extract full spectral characteristics of the anharmonic thermal motion of a microcantilever naturally vibrating at ambient temperature. Present work aims at the detection of comparatively noise free higher resonance modes and harmonics of thermal vibration for sensor applications without externally induced vibration. In microcantilever sensor based experiments with optical detection of cantilever deflection, we demonstrate the problems associated with the conventional procedure of processing photodetector signal for resonating microcantilevers and describe improvements. It has been experimentally demonstrated that isolation of the dynamic component of a position sensitive photodetector signal from its static counterpart significantly improves the resolution and limit of detection of an instrument. Outputs from conventional and proposed methods have been compared with experiments performed in both ambient air and liquid environments. A very simple and cost-effective circuit design is presented. © *2003 American Institute of Physics.* [DOI: 10.1063/1.1604953]

I. INTRODUCTION

There is a wide range of published work pertaining to the study of thermally induced vibrations of microcantilevers. The study of thermal noise spectra was initially of scientific importance because of the use of microcantilevers in atomic force microscopy (AFM).[1] Many such studies view the thermal noise as interference to obtaining optimum AFM images. The study of the ambient thermal noise of microcantilevers has been shown to help in determination of the spring constant of microcantilevers.[2–6] Thermal vibration of a microcantilever has also been found to be useful for physical, chemical and biological sensor applications.[7–21] As a sensor, the shift in resonance frequency of a microcantilever is detected as a result of interactions with the analyte or physical property of interest. It may be used for the detection of adsorption of analyte specific mass,[7,8,12,14,17,18] vapors,[15,19] gases, flavors,[16] measurement of viscosity,[22] and phase change.[14] However, more often detection and sensing of the resonance have become a limitation and challenge for practical microcantilever sensor devices and applications due to the very small amplitude of vibration of thermal resonance.[13] There have been studies that have manipulated and exploited microcantilever resonance changes in various ways to conform to an application.[23–25] Generally an external technique is used where the microcantilever is excited into its fundamental resonance frequency. While the above approach of exciting a microcantilever with a piezoelectric bimorph element swept through a range of driving frequencies has been a convention,[7,12,14,16,23] Mehta *et al.* have used the position sensitive photodetector (PSD) signal itself to excite the microcantilever by piezoelectric element through a variable gain amplifier and a phase shifter in feedback mode.[26–27] Neuzil *et al.*[13] have demonstrated the actuation of micromachined cantilevers by airflow in a different approach like a free reed in wind musical instruments. Without directly measuring and following an excitation technique, the troubles of reproducibility and poor resolution of thermal resonance peaks often make an experiment unsuccessful. The situation worsens when performing an experiment in liquid environment or with variation in temperature, with microcantilevers of high spring constants. Sometimes even the fundamental mode remains buried in the noise background.

Here we report processing of PSD signal response due to ambient thermal vibration to avail clean higher order resonance modes and harmonics of microcantilevers for sensor applications. In this approach the microcantilever is allowed to vibrate freely at its natural frequencies; left undisturbed from any sort of artificial excitation. External agitation may not be favored for many experiments where a good adhesion (stability and equilibrium) between sample and microcantilever surface is intended. It also invokes many unwanted modes due to the coupling of the holder with microcantilever substrate and piezobimorph. So instead of obtaining resonance frequency of the microcantilever itself, it may actually include resonance frequency of the microcantilever–substrate–holder–bimorph assembly. When estimation and control of the degree of excitation may be troublesome leading to damage of microcantilever itself (it may fly off), resonance of the coupled bodies may also blur actual resonance frequency of microcantilever.[24] Tuning may find a wide dynamical range of frequencies around the resonance eigenmode yielding hardly any appreciable change in amplitude of vibration. The thermal motion naturally favors the soft modes, thus, the acquisition and interpretation of microcan-

[a)]Author to whom correspondence should be addressed; electronic mail: mgeorge@matsci.uah.edu

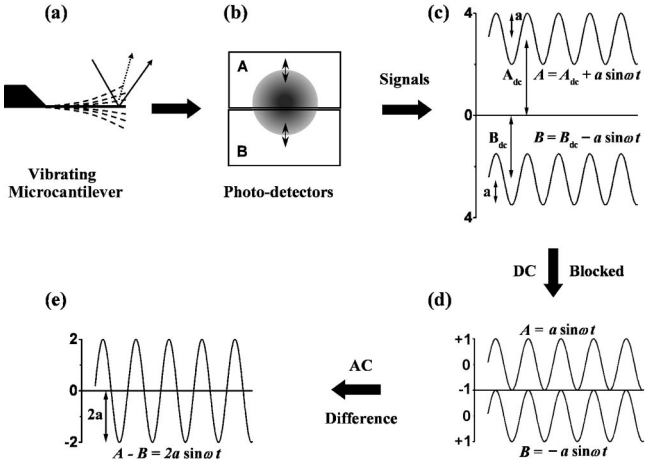

FIG. 1. Applied concept behind the operation on photodetector signals to extract alternating component.

tilever resonance spectra is simplified.[28] Higher order resonance modes are expected to demonstrate higher sensitivity to the change in experimental conditions.[29] They also enhance the sensitivity of atomic force microscopes operating in dynamical mode.[30,31] Higher modes may also improve determination of force constant of a microcantilever with less error.[5]

II. PHOTODETECTOR PROPERTIES

Common AFM heads are designed based on the optical lever technique where a laser beam is reflected back from the microcantilever to a PSD. The microcantilever itself is unstable. It may vibrate in different modes for its different degrees of freedom. Normally flexural or transverse modes of vibration are utilized in sensor applications and in tapping mode AFM. Microcantilever motion consists of two components, a relatively static deflection or bending due to externally induced conditions and a dynamic mechanical thermal vibration due to agitation from interactions with adjacent ambient molecules.[32] To collect the information on transverse deflection or vibration the difference of electrical signals of top and bottom parts of PSD is acquired. It is normalized and amplified in such a way that the spatial dynamical range of PSD fits within the saturation limit of amplifier. This is a mixed signal of direct and alternating components of PSD output voltage. So the amplifier operates within its saturation level for the amplification of both static and fluctuating PSD signals. This is the reason the dynamical signal ($\sim$ few tens of microvolts) is not amplified enough to be detected out of the noise background and most of the time remains buried within it.

In the present technique we employ a dedicated route for tracking fluctuating signals. The basic operational principle has been illustrated in Fig. 1. For simplicity we use a bicell photodiode with two parts, top A and bottom B [Fig. 1(b)]. The figure illustrates coexistence of alternating and direct components of voltage signals in the bicell PSD and the process of filtering out the ac signal from it. Due to the vibration of the microcantilever [Fig. 1 (a)], the spot of the laser beam on the PSD reflected from the microcantilever also oscillates [Fig. 1(b)]. It produces two signals simultaneously from A and B segments [Fig. 1(c)]. If the amplitude of vibration is **a** and the static deflections are $\mathbf{A_{dc}}$ and $\mathbf{B_{dc}}$ in A and B, respectively, as illustrated in Fig. 1(c), the amplitudes of oscillations in A and B at any instant of time t can be written as

$$A = A_{\mathrm{dc}} + a \sin \omega t, \tag{1}$$

and

$$B = B_{\mathrm{dc}} + a \sin(\omega t + \pi), \tag{2}$$

respectively. So the transverse signal means

$$A - B = (A_{\mathrm{dc}} - B_{\mathrm{dc}}) + 2a \sin \omega t. \tag{3}$$

Conventionally the detected signal is a normalized version of Eq. (3). Let us designate it to be the DCD signal, including the dc difference:

$$\mathrm{DCD\ signal} = \alpha \frac{A - B}{A + B}$$

$$= \frac{\alpha}{(A_{\mathrm{dc}} + B_{\mathrm{dc}})}[(A_{\mathrm{dc}} - B_{\mathrm{dc}}) + 2a \sin \omega t], \tag{4}$$

where α is an amplification factor. The first part in this equation gives static deflection or bending of microcantilever and the second part contains frequency information of thermal vibration of the microcantilever. To acquire clear information only on the vibration of the microcantilever the dc part can be suppressed allowing the ac part to have enough freedom to be amplified. For this purpose we utilize Eq. (3), avoiding normalization and assuming that the sum signal is fairly stable. We designate this to be the ACD signal, the signal of ac difference only:

$$\mathrm{ACD\ signal} = \beta(A - B) = 2a\beta \sin \omega t, \tag{5}$$

where β is the amplification factor. The difference doubles the amplitude keeping the frequency unchanged [Fig. 1(e)]. Technically first we have blocked dc of the signals from each segment [Fig. 1(d)] before their difference is taken. Equation (5) enhances the signal-to-noise (S/N) ratio, resulting in increased resolution of higher-order modes of vibration. The technique may be useful for any experimental setup for the detection and analysis of multiple vibration modes.

III. EXPERIMENT

PSD signals from a Digital Instruments MultiMode™ optical head were fed to two different ports, one is a standard DCD signal port and the other is for ACD signal. These were connected to an oscilloscope (TDS 3014B, Tektronix, Inc.) for analysis and recording microcantilever resonance characteristics. The basic electronics for isolation and detection of the ACD signal is shown in Fig. 2. The dc part of the signal from each segment of PSD was filtered and rejected individually through the dc-blocking circuits as illustrated in Fig. 1(d). Filtered signals were amplified to strengthen the vibrational signals against the background noise. Further amplification is done by passing signal through a differential ampli-

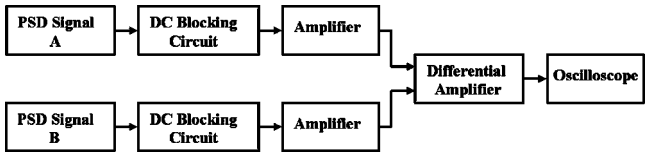

FIG. 2. A typical basic circuit block diagram for the amplification of vibrational modes of microcantilevers based on the operating principle described in Fig. 1.

fier. This results in a signal well above ($\sim$1000 times) the background noise level where the vibrational modes are buried.

This methodology was tested for three types of microcantilevers as described in Table I. Physical parameters of microcantilevers are as specified by the manufacturers. A standard metallic cantilever holder and a fluid–cell cantilever holder made of glass (Digital Instruments, Inc.) were used to study on cantilevers in air and water, respectively. Microcantilevers were allowed to vibrate freely at the tip–end in the absence of any sample surface to avoid tip–sample interaction.

IV. RESULTS AND DISCUSSION

A comparative study for the quality of signals obtained from the ACD and DCD ports has been performed in air and liquid environments. Each recorded spectrum represents a Fourier transform of a data sequence which is an average of 512 time sequences, each consisting of 10 000 sampling points.

Figure 3 shows a typical damping characteristic of a V-shaped microcantilever in ambient conditions recorded from the ACD port. It is relatively noise-free signal with clearly visible vibrational modes of the microcantilever. Motion of the microcantilever is a superposition of many eigenmodes of vibration. Higher frequency modes can be noticed within the envelope of lower frequency modes. Amplitude of vibrations is of the order of few volts. Root mean square (rms) values of these signals are at least 3 orders of magnitude higher than the values usually obtained from a standard DCD port. In our present setup, the DCD port yields signals of rms values usually varying from of the order of few 10 to a few 100 μV.

In ACD, the thermal resonance modes are found to be sustained in either air or in water; they are fairly stable and reproducible. The DCD signal was found to yield unstable

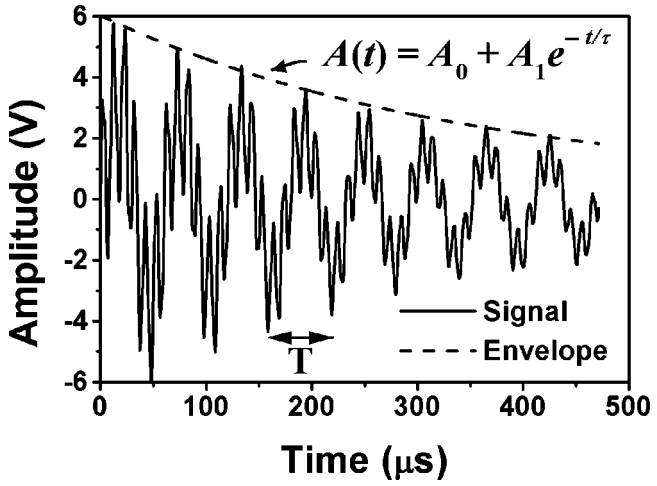

FIG. 3. Damped oscillations of a V-shaped microcantilever (sample No. 1) in air. $A(t)$ represents the decay profile of vibration; time period of the fundamental mode $T \approx 59\ \mu$s, $A_0 = 0.43$ V; $A_1 = 5.6$ V; decay time $\tau \approx 340\ \mu$s. It can be noticed that the profiles of higher frequency modes are guided by those of lower ones.

resonance peaks and most of the time they had highly transient appearance. This was particularly true when experimenting with variation in the temperature of the microcantilever, resonance frequencies almost disappear from DCD signal, but they continue in the ACD signal. However the ACD signal also shows instability over time; peaks disappear or gradually merge with the background but after a while they appear again.

The modified route has led to the detection of not only the fundamental and higher resonance modes but also some other modes which may be harmonics or may have some simple mathematical relationship with the fundamental or other resonance modes. The resonance characteristics of microcantilever No. 1 are illustrated in Fig. 4. Figure 3 is the time domain signal of Fig. 4(b). We see four prominent resonance modes in air together with some other modes in ACD when DCD shows the first three eigenmodes. Peaks at 34.2 and 51.4 kHz are the harmonics of the fundamental mode at 17.1 kHz, whereas the peak at 133 kHz is apparently unrelated to it. In water DCD shows three and ACD shows five peaks. In both cases the sharpness of peaks diminishes with increasing order. The first four modes at 4, 30, 91, and 184 kHz in Fig. 4(d) may correspond to the modes at 17.1, 99, 263, and 500 kHz in Fig. 4(b) with the corresponding reso-

TABLE I. Microcantilever samples used to test photodetector signals.

Microcantilever sample No.	Geometry[a]					Physical properties[b]			
	Shape	L	B	W	t	Material	f_1	k	Manufacturer
1	V-Shaped	193	205	20	0.6	Au-coated Si_3N_4	n/a[c]	0.06	Digital Instruments
2	Rectangular	300		35	1	Si	14	0.05	Ultrasharp
3	Rectangular	100		35	1	Si	125	1.2	Ultrasharp

[a] L = length (μm); B = breadth (μm); W = width (μm); and t = thickness (μm).
[b] f_1 = fundamental resonance frequency (kHz) and k = spring constant (N/m).
[c] n/a = not available.

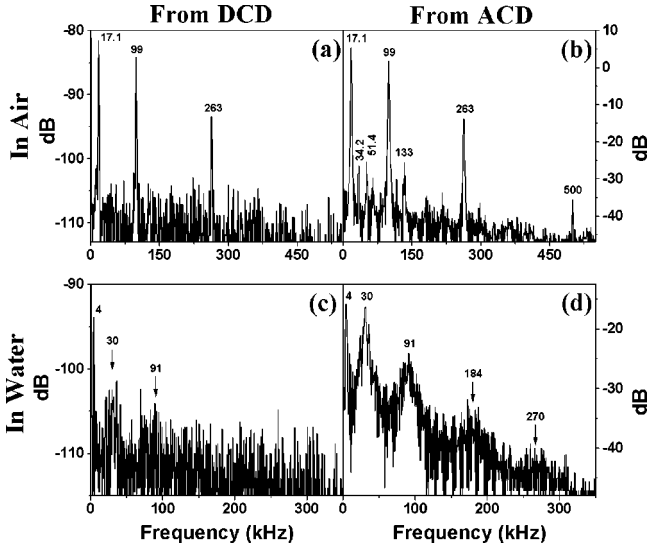

FIG. 4. Characteristic vibrational resonance modes of a V-shaped microcantilever (sample No. 1): (a)–(b) in air and (c)–(d) water. Clarity of acquired modes derived from only alternating components [(b), (d)] is better than that obtained from the unified form [(a), (c)] of photodetector signals. (b) shows appearance of two harmonics of the fundamental mode (17.1 kHz) together with other modes.

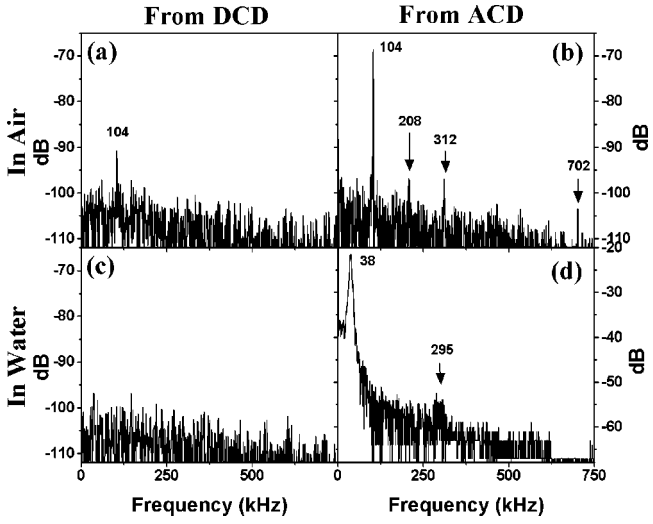

FIG. 6. Resonance modes of a comparatively high *k* rectangular microcantilever (sample No. 3): (a)–(b) in air and (c)–(d) in water; (a) and (c) from DCD and (b) and (d) from ACD port. The peaks at 208 and 312 kHz in (b) are two harmonics of the fundamental resonance mode at 104 kHz. 702 kHz is the second higher frequency flexural resonance mode.

nance shifts of 13.1, 69, 172, and 316 kHz, respectively.

More clear and informative data have been obtained from a comparatively low *k* rectangular microcantilever. In contrary to only two in air and no peaks in water in DCD signal, ACD yields at least 14 in air and five peaks in water (Fig. 5), for microcantilever No. 2. The four intense peaks at 12.4, 83, 237.5, and 469 kHz in air shown in Fig. 5(b) may correspond to the resonance peaks at 2.9, 24.4, 76.3, and 159.6 kHz in water shown in Fig. 5(d) with their corresponding shifts of 9.5, 58.6, 161.2, and 309.4 kHz, respectively. An important aspect of this experiment can be realized by comparing the DCD spectra of rectangular [Fig. 5(a)] and V shaped [Fig. 4(a)], microcantilevers in air. The latter looks less noisy than the former. The total reflected photon energy to the photodetector (relative sum signal) for a V-shaped microcantilever (8 V) was more than that for a rectangular one (3.8 V) for present experimental conditions. Still the spectrum out of ACD, Fig. 5(b), is very clean. Significance of this fact is that, for the same amount of reflected photon energy to the photodetector from a microcantilever, the ACD port possesses much cleaner information than the DCD port. The reason for the difference in photodetector sum signal is that the V-shaped microcantilever is gold coated and its free end has more reflecting surface area to the incident beam than that of a rectangular one.

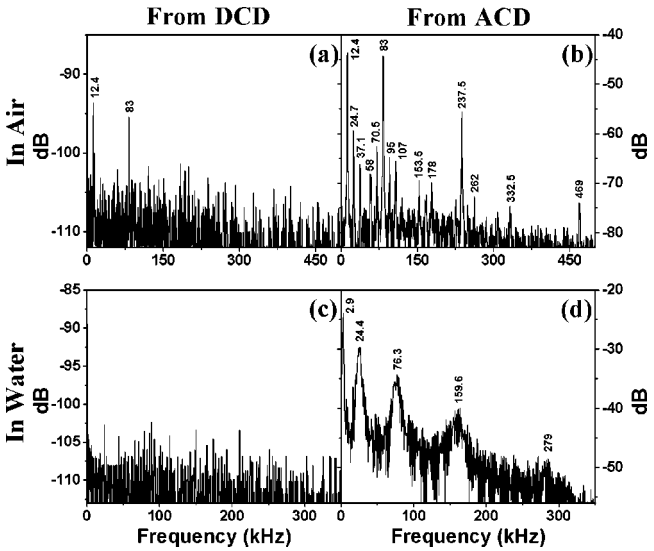

FIG. 5. Vibrational modes of a comparatively low *k* rectangular microcantilever (sample No. 2): (a)–(b) in air and (c)–(d) in water. Characteristics (a) and (c) are obtained from DCD and (b) and (d) from ACD port. ACD demonstrates a dramatic improvement for resolving and detecting higher harmonics and resonance modes of flexural vibrations.

Appearance of many other modes and harmonics can be noticed in Fig. 5(b). The prominent resonance modes at 12.4, 83, 237.5, and 469 kHz can be attributed to the flexural modes of the vibration of a microcantilever. Modes at 24.7 and 37.1 kHz are the second and third harmonics of the fundamental mode at 12.4 kHz. The rest of the modes may apparently have some simple mathematical relationship with the fundamental mode as discussed later.

The resonance characteristics of a relatively higher *k* microcantilever have been presented in Fig. 6. DCD hardly yields any resonance peak either in air or water. But ACD gives distinct features of vibration both in air and water. In air we clearly notice two harmonics at 208 and 312 kHz of the fundamental mode at 104 kHz, together with a higher resonance mode at 702 kHz. The characteristic peaks at 38 and 295 kHz in water may correspond to the peaks at 104 and 702 kHz in air with their shifts of 66 and 407 kHz, respectively.

Table II compares the qualitative characteristics of the signals measured at DCD and ACD ports for all the microcantilevers. *Q* factors and S/N ratios have been calculated for the fundamental mode from V-rms amplitude spectra. In-

TABLE II. Comparison of vibrational characteristic features of signals measured from ac and dc differences for the microcantilevers.

Microcantilever sample No.	Media	From DCD			From ACD		
		Number of modes	Q[a]	S/N	Number of modes	Q[a]	S/N
1	Air	3	8.6	31.6	~7	6.1	44.7
	Water	3	3.6	11.1	5	2.4	22.5
2	Air	2	19.6	14.9	~14	11.4	51
	Water	0	···	···	5	1.4	18.7
3	Air	1	51	16.5	4	14.8	47.8
	Water	0	···	···	2	1.6	36.1

[a]$Q=f_1/\Delta f$ is the quality factor, Δf is full width at half maxima.

crease in S/N is consistent with the increase in number of acquired modes in ACD with respect to DCD. Though Q factors should remain the same for both types of measurements, the apparent higher values of DCD can be attributed to higher background noise. Q values are displayed here only for information to have an idea about the intensity of resonance peaks but not as a figure of merit of any port. As the agitation and hence the vibration of a microcantilever is primarily Brownian type, its amplitude of oscillation is never stable. So the amplitude of characteristic peaks in fast Fourier transformed spectra also varies considerably, providing any reproducible Q value. ACD circuitry amplifies the rms amplitude by orders. In turn it enhances the clarity of the oscillatory signal but not the energy of vibration of a microcantilever, enabling detection and resolution of many other modes of vibration. This comparatively noise free amplified signal can be feedback to an integrated piezoelement to amplify AFM or the sensor signal if required for an application. However amplification of the signal at the DCD port reduces the signal to noise ratio.

Resonance frequency values of microcantilevers have been checked with a MultiMode-SPM (Nanoscope-III, Digital Instruments, Inc.) setup, where they have been forced to vibrate over a wide range of driving frequencies induced by a piezoelectric element. The result is furnished in Table III. It shows a fair agreement between the values obtained from different methods. The resonance frequency of each normal mode of vibration for an undamped rectangular cantilever with one end free can be expressed by[23,33]

$$f_i=\frac{t}{4\pi}\left(\frac{\alpha_i}{L}\right)^2\sqrt{\frac{Y}{3\rho}}, \tag{6}$$

where $\alpha_i=1.875$, 4.694, 7.855, 10.996 for $i=1$, 2, 3, 4, respectively; indices correspond to different modes of vibration, for higher values of i, $\alpha_i\approx(i-1/2)\pi$; L, Y, and ρ stand for length, Young's modulus, and density of the microcantilever, respectively. To verify the frequencies of flexural modes of vibration of rectangular microcantilevers, we have further calculated them using Eq. (6) assuming $Y=1.79\times10^{11}$ N/m and $\rho=2330$ kg/m^3. These are also shown in Table III for comparison. Calculated values deviate considerably from the experimental values. This may be due to the deviation of assumed or gross values of all physical and geometrical parameters from their exact values and effects of viscous damping in air. However a qualitative idea can be gathered from these calculated values about their positions in the resonance spectra and confirming the origin of experimental values to be the resonance eigenmodes of vibration.

In ACD spectra there are some peaks associated with the resonance modes in air, which may have some simple mathematical relationship with the resonance eigenvalues. Each resonance mode together with the peaks distributed evenly in its proximity forms a group. The first group of peaks can be written as nf_1, where n is the order of harmonics. In Figs. 4(b), 5(b), and 6(b) they are the first three peaks marked with their frequency values. Other groups of frequencies in the spectra can be represented by: $f_i\pm(m-1)f_1$, where $i=2$, 3, 4 etc., order of different resonance modes; $m=1$, 2, 3 etc. the indices of other modes centering a higher resonance mode. We find that the difference of frequencies of any two members within a group is an integer multiple of fundamental resonance frequency within the error limit. Let us define them to be differential harmonics against the usual harmonics in the first group. This is more obvious in Fig. 5(b) than Fig. 4(b). Harmonics with higher amplitude are closer to a resonance mode. Amplitudes of harmonics gradually die out on both the lower and higher frequency side of the mode.

Anharmonic motion of the cantilever generates fre-

TABLE III. Comparison of the values of thermal resonance eigenfrequencies obtained from different methods in air.

Microcantilever sample No.	Resonance frequencies (kHz) from		
	ACD	DI Nanoscope-III	Eq. (6)
1	17.1, 99, 263, 500	15.4, 89.7, 276.5, 490.9	···
2	12.4, 83, 237.5, 469	12.3, 82.3, 236.5, 467.2	15.8, 98.4, 275.7, 541.4
3	104, 702	103.8, 701	142.3, 885.8

quency components concentrating in harmonics and differential harmonics around the resonance eigenmodes. Members of a group except in the first group are not harmonics of the fundamental resonance frequency, as it happens when the microcantilever undergoes harmonic distortion by tip–sample interaction potential in tapping mode AFM operation.[34] We do not know the exact reason for the origin of these peaks. Nonlinear tip–sample interaction is thought to be the main reason.[35,36] This may be a secondary reason, differential harmonics are further excited or at best disturbed by the nonlinear tip–sample interaction potential. The resonance spectrum of a microcantilever in air is definitely a signature of an anharmonic oscillator like a molecule. We speculate that the primary cause of the origin of these differential harmonics is hidden within the microcantilever itself. As a microelectromechanical system device it behaves like a gigantic molecule. The groups of frequencies may be its molecular energy states of vibration.

Presented data may not be at best experimental condition and do not represent the ultimate and exhaustive results of the suggested method. These are rather qualitative information of our preliminary design and experiments signifying its possibility. The quality of signal depends upon many factors like the circuit components itself, ability of signal analyzer, optical alignment, shape and reflectivity of microcantilever, nonlinearity of detector sensitivity, vibration isolation, etc., which require care to have noise free intensified and clean signal. A subtle change of any of these factors may reduce the signal quality considerably. Appearance or disappearance of the harmonics depends very much on the influence of random environmental fluctuations on the microcantilever.

V. CONCLUSION

It is very important to isolate and discard the static component of a photodetector signal to enhance the resolution and sensitivity of an instrument of sensor application. Only the alternating component of detector signal substantially enhances the quality of experimental results. The process can detect and resolve higher order resonance eigenmodes and many harmonics hidden within the natural Brownian motion of a microcantilever. Our proposition is if the static deflection is redundant in any experiment it should be rejected, otherwise if it carries desired information one should make a separate channel for the same. It may be possible to perform many sensor based microcantilever experiments without the necessity of external excitation. The method is cost-effective and can be implemented in the laboratory without the need for other instrumentation.

ACKNOWLEDGMENT

This work is supported by NASA EPSCoR Grant No. NCC5-580.

[1] D. O. Koralek, W. F. Heinz, M. D. Antonik, A. Baik, and J. H. Hoh, Appl. Phys. Lett. **76**, 2952 (2000).
[2] J. P. Cleveland, S. Manne, D. Bocek, and P. K. Hansma, Rev. Sci. Instrum. **64**, 403 (1993).
[3] J. L. Hutter and J. Bechhoefer, Rev. Sci. Instrum. **64**, 1868 (1993).
[4] J. E. Sader, J. W. M. Chon, and P. Mulvaney, Rev. Sci. Instrum. **70**, 3967 (1999).
[5] J. Colchero, in *Procedures in Scanning Probe Microscopies*, edited by R. J. Colton *et al.* (J. Wiley, Chichester, 1998), pp. 133–138.
[6] J. E. Sader, I. Larson, P. Mulvaney, and L. R. White, Rev. Sci. Instrum. **66**, 3789 (1995).
[7] G. Y. Chen, T. Thundat, E. A. Wachter, and R. J. Warmack, J. Appl. Phys. **77**, 3618 (1995).
[8] T. Thundat, E. A. Wachter, S. L. Sharp, and R. J. Warmack, Appl. Phys. Lett. **66**, 1695 (1995).
[9] R. Raiteri, M. Grattarola, H.-J. Butt, and P. Skládal, Sens. Actuators B **79**, 115 (2001).
[10] R. Raiteri, M. Grattarola, and R. Berger, Mater. Today, **5**, 22 (2002).
[11] T. Thundat, P. I. Oden, and R. J. Warmack, Microscale Thermophys. Eng. **1**, 185 (1997).
[12] P. I. Oden, Sens. Actuators B **53**, 191 (1998).
[13] P. Neuzil, U. Sridhar, and B. IIic, Appl. Phys. Lett. **79**, 138 (2001).
[14] E. A. Wachter and T. Thundat, Rev. Sci. Instrum. **66**, 3662 (1995).
[15] R. Raiteri, S. Martinoia, F. Molinari, G. Carlini, D. Ricci, and M. Grattarola, in *Proceedings of the Third Italian Conference on Sensors and Microsystems*, Genova, Italy (World Scientific, Singapore, 1998).
[16] H. P. Lang, M. K. Baller, R. Berger, Ch. Gerber, J. K. Gimzewski, F. M. Battiston, P. Fornaro, J. P. Ramseyer, E. Meyer, and H. J. Güntherodt, Anal. Chim. Acta **393**, 59 (1999).
[17] R. Berger, Ch. Gerber, H. P. Lang, and J. K. Gimzewski, Microelectron. Eng. **35**, 373 (1997).
[18] T. Thundat, R. J. Warmack, G. Y. Chen, and D. P. Allison, Appl. Phys. Lett. **64**, 2894 (1994).
[19] P. G. Datskos and I. Sauers, Sens. Actuators B **61**, 75 (1999).
[20] S. Cherian and T. Thundat, Appl. Phys. Lett. **80**, 2219 (2002).
[21] G. Y. Chen, R. J. Warmack, T. Thundat, D. P. Allison, and A. Huang, Rev. Sci. Instrum. **65**, 2532 (1994).
[22] P. I. Oden, G. Y. Chen, R. A. Steele, R. J. Warmack, and T. Thundat, Appl. Phys. Lett. **68**, 3814 (1996).
[23] D. Sarid, *Scanning Force Microscopy: With Applications to Electric, Magnetic and Atomic Forces*, 2nd ed. (Oxford University Press, New York, 1994).
[24] J. Tamayo, A. D. L. Humphris, and M. J. Miles, Appl. Phys. Lett. **77**, 582 (2000).
[25] T. R. Albrecht, P. Grütter, D. Horne, and D. Rugar, J. Appl. Phys. **69**, 668 (1991).
[26] A. Mehta, S. Cherian, D. Hedden, and T. Thundat, Appl. Phys. Lett. **78**, 1637 (2001).
[27] G. Muralidharan, A. Mehta, S. Cherian, and T. Thundat, J. Appl. Phys. **89**, 4587 (2001).
[28] D. A. Walters, J. P. Cleveland, N. H. Thomson, P. K. Hansma, M. A. Wendman, G. Gurley, and V. Elings, Rev. Sci. Instrum. **67**, 3583 (1996).
[29] M. Hoummady and E. Farnault, Appl. Phys. A: Mater. Sci. Process. **66**, S361 (1998).
[30] U. Rabe, J. Turner, and W. Arnold, Appl. Phys. A: Mater. Sci. Process. **66**, S277 (1998).
[31] Ch. Loppacher, M. Bammerlin, F. Battiston, M. Guggisberg, D. Müller, H. R. Hidber, R. Lüthi, E. Meyer, and H. J. Güntherodt, Appl. Phys. A: Mater. Sci. Process. **66**, S215 (1998).
[32] J. R. Vig and Y. Kim, IEEE Trans. Ultrason. Ferroelectr. Freq. Control **46**, 1558 (1999).
[33] H.-J. Butt and M. Jaschke, Nanotechnology **6**, 1 (1995).
[34] R. Hillenbrand, M. Stark, and R. Guckenberger, Appl. Phys. Lett. **76**, 3478 (2000).
[35] J. Tamayo, Appl. Phys. Lett. **75**, 3569 (1999).
[36] R. W. Stark and W. M. Heckl, Surf. Sci. **457**, 219 (2000).